PHYSICAL REVIEW B **66**, 220102(R) (2002)

Orientation dependence of shock-induced chemistry in diamond

S. V. Zybin,[1] M. L. Elert,[2] and C. T. White[3,*]
[1]*Department of Chemistry, The George Washington University, Washington, D.C. 20052*
[2]*Chemistry Department, U.S. Naval Academy, Annapolis, Maryland 21402-5026*
[3]*Naval Research Laboratory, Washington, D.C. 20375-5320*
(Received 17 August 2002; published 18 December 2002)

Molecular dynamics simulations employing a reactive empirical bond order potential are used to study the orientational dependence of shock-induced chemistry in diamond. Even for strong shock waves, the mechanism of bond breaking and shock-induced transition to amorphous carbon is found to depend crucially on the direction of shock wave propagation. For ⟨110⟩ oriented shock waves, high rate shear deformation causes the formation of layered carbon structures while ⟨111⟩ shock waves favor the formation of diamond micrograins separated by amorphous carbon inclusions.

DOI: 10.1103/PhysRevB.66.220102 PACS number(s): 62.50.+p, 82.40.Fp, 81.30.Hd, 46.40.Cd

A better understanding of the orientational dependence of shock waves in solids could prove key in unraveling the initial stages of shock-induced chemistry important in developing insensitive explosives.[1,2] Already molecular dynamics (MD) simulations of shock waves in rare-gas solids have shown significant orientation dependence of the shock front structure in these materials.[3,4] However, there have been few simulations showing any significant effects of shock wave orientation on the breaking and making of covalent bonds. A good candidate for initial study is diamond with its highly directed covalent bonding. Indeed, density-functional calculations of diamond lattice instabilities and cleavage,[5,6] and elastic properties,[7–9] as well as tight-binding studies of diamond under uniaxial static tension,[10] have shown significant orientation effects in diamond lattice failure.

Unfortunately, first-principles and tight-binding methods cannot currently be used to directly simulate shock-induced failure of solids because of the large number of atoms, which must be included to capture the formation of extended defects. Atomistic MD simulations using classical potentials have proven to be able to include enough atoms for long enough times to treat complex behaviors such as melting,[3] plastic deformations,[4,11] simple detonations,[12–14] and shock wave splitting caused by phase transitions[15,16] and elastic-plastic transformations.[4,13] However, any simulations of strong shocks in diamond must employ a potential that includes a variety of chemical effects including bond-breaking and bond-making reactions and the tendency of carbon to form $sp^n (n=1-3)$ bonds of different relative orientations and strengths in different environments. Herein, we report on the results from a study of the orientational dependence of strong shock waves in diamond using a carbon reactive empirical bond order (REBO) potential that does have these essential ingredients.

The carbon REBO potential was originally developed to study diamond chemical vapor deposition[17] and subsequently used in the simulation of a broad range of carbon-based systems,[18–20] including studies of the diamond melting line and the liquid-liquid carbon phase transition.[21] Recently it has been modified to better reproduce diamond elastic properties,[22] and successfully applied to simulate the fracture of polycrystalline diamond.[23]

Our diamond simulations were performed within the shock front reference frame by maintaining the front at rest in a computational box. Periodic boundary conditions were applied in the transverse x and y directions with the z axis of shock wave propagation oriented along either the ⟨110⟩ direction or ⟨111⟩ direction in the diamond sample. The sample, at an initial temperature of 300 K, contained $\approx 90\,000$ atoms at a density $\rho_0 = 3.52$ g/cm^3 with transverse dimensions of 5×5 nm. The shock front was maintained at rest in the computational box by adjusting the piston velocity u_p for a given shock (box) velocity u_s. This approach has shown significant advantages over methods of shock simulation within the material or piston reference frame in the accuracy of fine-grid shock profiles and distribution functions.[11] However, it cannot be used to study shock wave splitting that leads to two shock fronts moving at different velocities. This limitation motivates our choice of u_s far enough above the elastic-plastic breakpoint on the Hugoniot to obtain a single stable plastic shock wave.

Figure 1 depicts two instantaneous views of a ⟨111⟩ shock wave with the bonds shaded according to the local potential energy per atom. Only a few y-z and x-z planes taken from the sample are shown for clarity. Clearly visible is the shock-induced breakup of the diamond structure through formation of amorphous carbon inclusions separating diamondlike micrograins. The pressure $P_s \approx 900$ GPa and temperature $T_s \approx 13\,000$ K of the compressed material behind the shock front lie close to the calculated continuation of the experimental Hugoniot[24] into the liquid phase above the latest diamond melting curve.[25]

A similar simulation at much the same piston velocity was performed for a shock wave oriented along the ⟨110⟩ direction in the sample. Time-averaged profiles[26] of the mass velocity u_z and potential energy E_p for this ⟨110⟩ shock wave, together with the corresponding profiles for the ⟨111⟩ shock wave depicted in Fig. 1, are shown in Fig. 2. Profiles of both the ⟨110⟩ and ⟨111⟩ shock waves exhibit an oscillatory structure at the leading edge of the shock layer corresponding to a region of elastic compression. These oscillations, also observed in MD simulations of rare-gas crystals,[11] originate from collisions of atomic planes in the z direction as in a one-dimensional chain. Even for these strong shock waves,

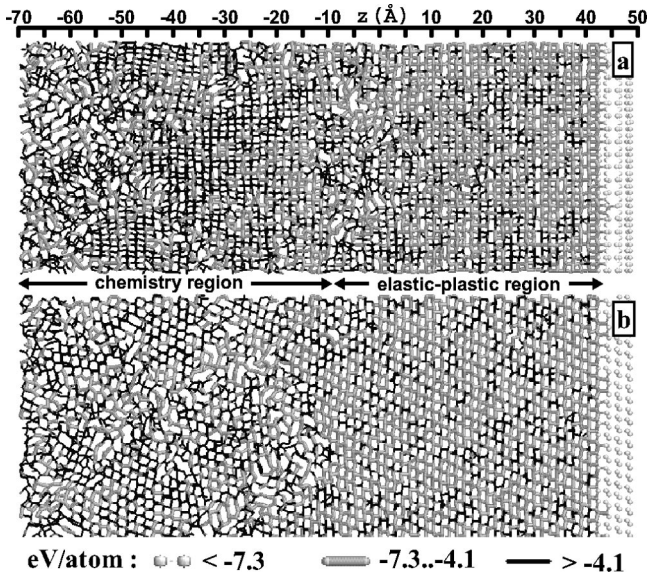

FIG. 1. Snapshot of a ⟨111⟩ diamond shock wave with $u_p = 9.2$ km/sec, where (a) y-z planes and (b) x-z planes are depicted.

plastic deformations cannot develop instantly, but rather require some time for the shear stress to achieve a critical value. After the oscillations fade and the shear stress achieves its sustained maximum value, plastic deformation develops. These elastic regions do not enlarge with increasing time, because the shock waves are overdriven with respect to the elastic-plastic transition and hence no shock wave splitting occurs.

Figure 3 displays time-averaged profiles of the longitudinal component of the stress tensor σ_{zz} and the shear stresses τ_{xz} and τ_{yz}, calculated using Irving-Kirkwood formulas.[27] While the shear stresses are equal in the ⟨111⟩ shock wave, they are different for the ⟨110⟩ orientation. This difference arises because of the highly directed covalent bonding that complicates the mechanism of shock-induced plasticity of diamond in comparison to previously studied rare-gas solids. However, the shear stresses in both directions are quickly approaching zero, indicating the initiation of melting.

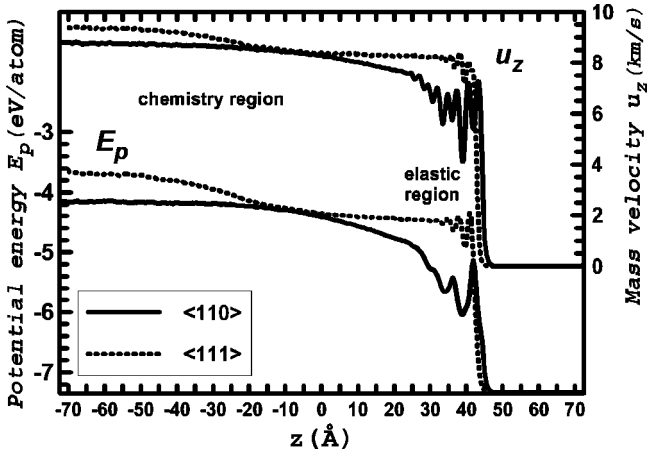

FIG. 2. Time-averaged ⟨110⟩ and ⟨111⟩ shock wave profiles at $u_p = 8.8$ and 9.2 km/s, $u_s = 30$ and 31 km/s, and compression ratios $\rho_0/\rho_s \approx 0.71$ and 0.70, respectively.

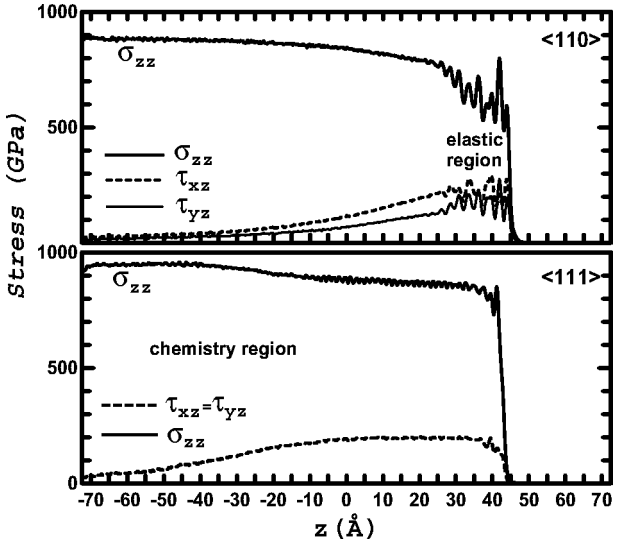

FIG. 3. Time-averaged ⟨110⟩ and ⟨111⟩ pressure profiles for the shock waves of Fig. 2. Shear stresses are $\tau_{xz} = \frac{1}{2}(\sigma_{zz} - \sigma_{xx})$ and $\tau_{yz} = \frac{1}{2}(\sigma_{zz} - \sigma_{yy})$.

To compare the structure of the resulting carbon phases in the shock layer behind the elastic region, we calculated the coordination and bond angle distributions for carbon atoms within a slab, where bond breaking and making (chemistry) are occurring. The results shown in Fig. 4 indicate a significant orientational dependence in the carbon phases obtained immediately behind the elastic shock region. When amorphization begins, sp^2-bonded atoms dominate the chemistry region in the ⟨110⟩ shock wave while the ⟨111⟩-oriented shock wave retains a relatively large number of fourfold coordinated carbons. Recently, the possibility of transformation from diamond to amorphous carbon containing a significant amount of sp^2-bonded atoms has been reported in indentation experiments[28] that produce a combination of shear and hydrostatic stress. Density-functional calculations[6] have also shown that graphitization of diamond due to applied shear stress is expected to be highly anisotropic.

Additional simulations of overdriven shock waves were performed to see if lower piston velocities would affect the

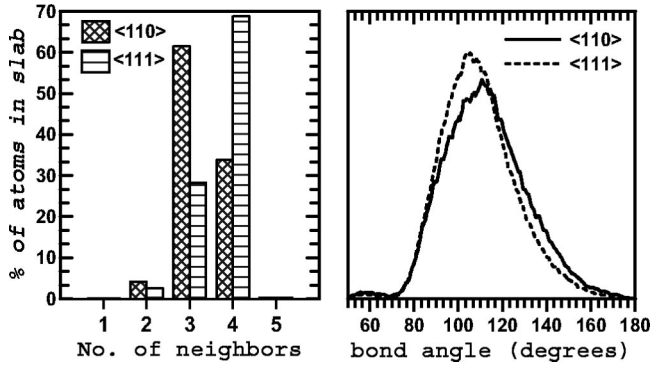

FIG. 4. Coordination number and normalized bond angle distributions for carbon atoms in a slab extending from $z = -70$ to -20 Å in Fig. 1. The $sp^2[sp^3]$ carbons should be threefold [fourfold] coordinated with bond angles tending to 120°[109.5°].

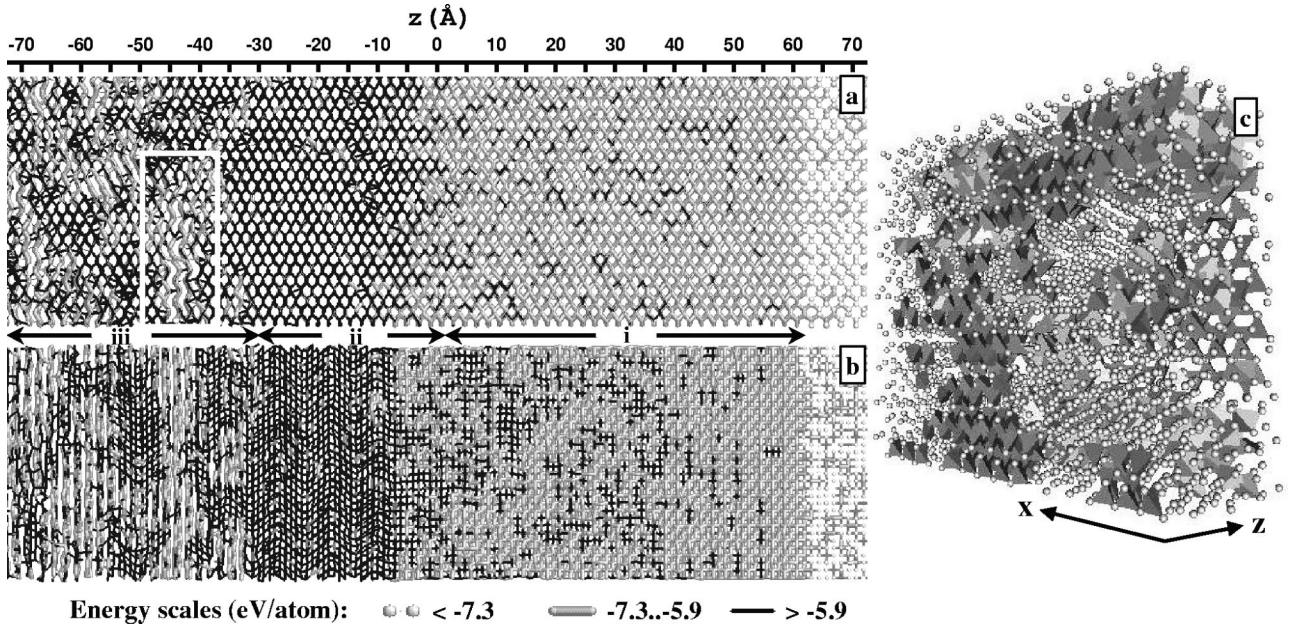

FIG. 5. Snapshot of ⟨110⟩ shock wave in diamond for $u_p = 6.1$ km/s, $u_s = 25$ km/s, and $\rho_0/\rho_s \approx 0.76$, where (a) y-z planes and (b) x-z planes are depicted; (c) shows sp^3 bond breaking and formation of graphitelike layered structures in the rectangle inset of (a). Atoms in (a) and (b) are shaded according to the potential-energy scales shown at the bottom of the figure.

results. However, we found that ⟨111⟩ shock waves become unsteady at piston velocities lower than 8 km/s, presumably due to shock wave splitting. Significantly, weaker overdriven ⟨110⟩ shock waves were, however, found steady enough to study by using our stationary shock frame technique. Figure 5 depicts a typical snapshot of atomic planes within the shock layer for a ⟨110⟩ shock wave corresponding to a piston velocity of $u_p = 6.1$ km/sec. The results are again shaded by the the potential energy per atom across the shock layer. Time-averaged profiles of the mass velocity u_z and the potential energy E_p for this moderately overdriven shock wave are shown in Fig. 6.

The shock layer now consists of three easily distinguishable regions: (i) an elastic region, (ii) a shear region, and (iii) a chemistry region. The elastic region again exhibits a steady oscillatory profile ahead of an overdriven plastic wave. This oscillatory structure, although more pronounced and of greater length than the corresponding structure seen in Fig. 2, remains pinned to the plastic wave. Then, within the shear region, a zigzag deformation develops in the x-z planes but not in the y-z planes as can be seen in Fig. 5. This zigzag pattern causes a lattice instability perpendicular to the direction of shock propagation. It is followed by sp^3-bond breaking resulting in the formation of graphitelike layered carbon structures. These layers are clearly visible within the chemistry region in Fig. 5(b), where only a few parallel x-z planes are depicted. Notice that the atoms in the layers have relatively lower potential energy per atom due to the formation of the graphitic structures. This decrease of the average potential energy within a region of π bonding can also be seen in Fig. 6. The resulting structure is highlighted in the small rectangular inset of Fig. 5(a). There only tetrahedral bonds (indicated by tetrahedrons) are depicted to emphasize their breakage.

Time-averaged stress profiles corresponding to Fig. 6 are plotted in Fig. 7. The shear stresses τ_{xz} and τ_{yz} are now not only unequal within the shock layer but also relax differently. Specifically, τ_{yz} is noticeably relaxed by the zigzag move-

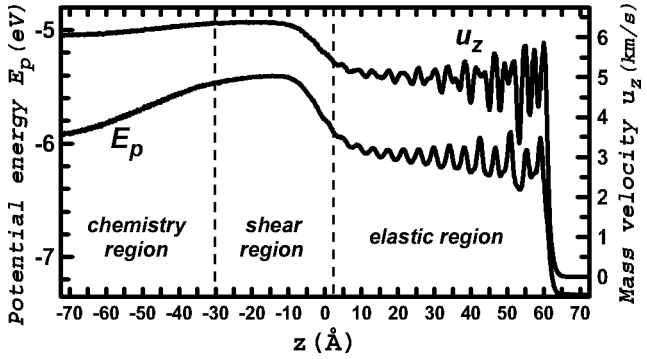

FIG. 6. Time-averaged profiles of $E_p(z)$ and $u_z(z)$ for a ⟨110⟩ shock wave with $u_p = 6.1$ km/s and $u_s = 25$ km/s.

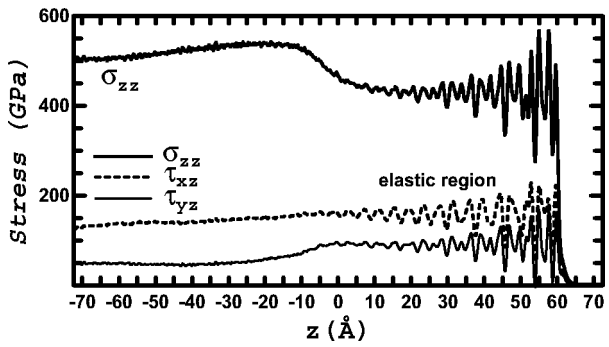

FIG. 7. Time-averaged ⟨110⟩ stress profiles for the shock wave in Fig. 6.

ment of neighboring x-y planes within the shear region, while τ_{xz} is only slightly decreased over the entire region. The shear stresses no longer approach zero because the pressure $P_s \approx 500$ GPa and temperature $T_s \approx 7000$ K in the compressed amorphous carbon phase remain below the melting transition.

In contrast to $\langle 111 \rangle$ and $\langle 110 \rangle$ oriented shock waves, we have failed to obtain shock-induced bond breaking for $\langle 100 \rangle$ oriented shock waves even for a strong compression ratio up to $\rho_0/\rho_s = 0.65$. This difference in the simulated shock responses arises because internal strain, which favors static displacements of lattice atoms in the lateral directions for $\langle 110 \rangle$ and $\langle 111 \rangle$ compressions, does not exist in the $\langle 100 \rangle$ case for any compression ratio; stretching of one bond compresses other equivalent bonds due to symmetry. Hence, shear deformation and slippage—hampered by the absence of preexisting defects—require longer times to develop. Because the time of passage of atoms through our stationary frame is about a picosecond, we are unable to observe a longer-time plastic response in our MD shock experiments. An anomalous elastic response to $\langle 100 \rangle$ shock compression has been also reported in silicon.[29] In addition, plastic flow and melting have been found harder to induce in MD simulations of $\langle 100 \rangle$ shock waves in rare-gas fcc solids.[3,4]

Taken together, the results reported in this paper show a significant orientation dependence of shock-induced chemistry in diamond even for strong shock waves.

This work was supported by ONR. We thank V.V. Zhakhovskiĭ, J.A. Harrison, and G.T. Gao for discussions.

*Electronic address: carter.white@nrl.navy.mil

[1] J.J. Dick, J. Phys. Chem. **97**, 6193 (1993).
[2] C.S. Yoo, N.C. Holmes, P.C. Souers, C.J. Wu, F.H. Ree, and J.J. Dick, J. Appl. Phys. **88**, 70 (2000).
[3] V.V. Zhakhovskiĭ, S.V. Zybin, K. Nishihara, and S.I. Anisimov, Suppl. Prog. Theor. Phys. **138**, 223 (2000).
[4] T.C. Germann, B.L. Holian, P.S. Lomdahl, and R. Ravelo, Phys. Rev. Lett. **84**, 5351 (2000).
[5] R.H. Telling, C.J. Pickard, M.C. Payne, and J.E. Field, Phys. Rev. Lett. **84**, 5160 (2000).
[6] H. Chacham and L. Kleinman, Phys. Rev. Lett. **85**, 4904 (2000).
[7] O.H. Nielsen, Phys. Rev. B **34**, 5808 (1986).
[8] A. Fukumoto, Phys. Rev. B **42**, 7462 (1990).
[9] J.-J. Zhao, S. Scandolo, J. Kohanoff, G. Chiarotti, and E. Tosatti, Appl. Phys. Lett. **75**, 487 (1999).
[10] Y. Uemura, Phys. Rev. B **51**, 6704 (1995); **49**, 6528 (1994).
[11] V.V. Zhakhovskiĭ, S.V. Zybin, K. Nishihara, and S.I. Anisimov, Phys. Rev. Lett. **83**, 1175 (1999).
[12] C.T. White, D.H. Robertson, M.L. Elert, and D.W. Brenner, in *Microscopic Simulations of Complex Hydrodynamic Phenomena*, edited by M. Mareschal and B.L. Holian (Plenum Press, New York, 1992), p. 111.
[13] D.H. Robertson, D.W. Brenner, and C.T. White, in *High Pressure Shock Compression of Solids III*, edited by L. Davison and M. Shahinpoor (Springer, New York, 1998), p. 37.
[14] D.W. Brenner, D.H. Robertson, M.L. Elert, and C.T. White, Phys. Rev. Lett. **70**, 2174 (1993).
[15] D.H. Robertson, D.W. Brenner, and C.T. White, Phys. Rev. Lett. **67**, 3132 (1991).
[16] K. Kadau, T.C. Germann, P.S. Lomdahl, and B.L. Holian, Science **296**, 1681 (2002).
[17] D.W. Brenner, Phys. Rev. B **42**, 9458 (1990).
[18] D.W. Brenner, J.A. Harrison, C.T. White, and R.J. Colton, Thin Solid Films **206**, 220 (1991).
[19] B.I. Dunlap, D.W. Brenner, J.W. Mintmire, R.C. Mowrey, and C.T. White, J. Phys. Chem. **95**, 5763 (1991).
[20] J.A. Harrison, C.T. White, R.J. Colton, and D.W. Brenner, Phys. Rev. B **46**, 9700 (1992).
[21] J.N. Glosli and F.H. Ree, J. Chem. Phys. **110**, 441 (1999); Phys. Rev. Lett. **82**, 4659 (1999).
[22] D.W. Brenner, O.A. Shenderova, J.A. Harrison, S.J. Stuart, B. Ni, and S.B. Sinnott, J. Phys.: Condens. Matter **14**, 783 (2002).
[23] O.A. Shenderova, D.W. Brenner, A. Omeltchenko, X. Su, and L.H. Yang, Phys. Rev. B **61**, 3877 (2000).
[24] M. Pavlovskii, Sov. Phys. Solid State **13**, 741 (1971).
[25] K.V. Khishchenko, V.E. Fortov, I.V. Lomonosov, M.N. Pavlovskii, G.V. Simakov, and M.V. Zhernokletov, in *Shock Compression of Condensed Matter*, edited by M. D. Furnish, N. N. Thadhani, and Y. Horie, AIP Conf. Proc. No. 620 (AIP, Melville, NY, 2002), p. 759.
[26] Profiles were obtained by averaging over ≈ 0.5 ps. Doubling this time leads to little change in the results.
[27] R.J. Hardy, J. Chem. Phys. **76**, 622 (1982).
[28] Y.G. Gogotsi, A. Kailer, and K.G. Nickel, J. Appl. Phys. **84**, 1299 (1998); Nature (London) **401**, 663 (1999).
[29] A. Loveridge-Smith *et al.*, Phys. Rev. Lett. **86**, 2349 (2001).